

Orbital Magnetism and Magnetic Anisotropy Probed with Ferromagnetic Resonance

A. N. Anisimov, M. Farle,* P. Pouloupoulos, W. Platow, and K. Baberschke

Institut für Experimentalphysik, Freie Universität Berlin, Arnimallee 14, D-14195 Berlin-Dahlem, Germany

P. Isberg,† R. Wäppling, A. M. N. Niklasson, and O. Eriksson

Department of Physics, Uppsala University, Box 530, S-75121 Uppsala, Sweden

(Received 27 July 1998)

Via ferromagnetic resonance both the magnetic anisotropy energy (MAE) and the spectroscopic splitting tensor (g tensor) for a bcc $\text{Fe}_2/\text{V}_5(001)$ superlattice are measured independently. The theoretically proposed proportionality between the anisotropy of the orbital moment μ_L and the MAE is quantitatively checked and its limitations are discussed. From layer-resolved *first-principles* calculations we find a reduced spin moment $\mu_S = 1.62\mu_B$ for Fe and $\mu_S^V = -0.67\mu_B$ in the first V layer. The g -tensor elements reveal a 300% enhanced ratio $\mu_L/\mu_S = 0.133$ in comparison to bulk Fe. The MAE and the orbital moment anisotropy is found to be unusually small for Fe monolayers. [S0031-9007(99)08741-4]

PACS numbers: 75.70.Ak, 75.30.Gw, 75.30.Pd

For a long time the magnetism of $3d$ metals has been described only in terms of spin magnetism. The relativistic spin-orbit interaction which leads to orbital magnetism and is manifested in the existence of magnetic anisotropy energy (MAE) was neglected. This has been justified by reasoning that due to the high symmetry of bulk crystals the orbital contribution is nearly completely quenched. Later in extending the localized models of ionic crystals to band ferromagnets Bruno [1] calculated within second-order perturbation theory at $T = 0$ K that the MAE is related to the difference $\Delta\mu_L = \mu_L^\perp - \mu_L^\parallel$ of orbital moments with respect to the symmetry axis of the crystallographic lattice,

$$\text{MAE} = -\alpha \frac{\lambda}{4\mu_B} \Delta\mu_L, \quad (1)$$

with the spin-orbit coupling parameter $\lambda = -0.054$ eV [1] for Fe. More recent *first-principles* calculations [2–5], on the other hand, have shown that a strict proportionality between MAE and $\Delta\mu_L$ does not exist (see, for example, Fig. 5 of [2]). Thus it is questionable to deduce the magnitude of MAE from a determination of anisotropic orbital moments. In ultrathin films the MAE and orbital moment anisotropy are enhanced, since tetragonally distorted lattices with partially unquenched μ_L [2,6] are stabilized. Both orbital μ_L and spin μ_S moments have been determined in x-ray magnetic circular dichroism (XMCD) experiments [7] by applying the sum rules. In this analysis which uses a localized picture the results have been interpreted as an enhancement or anisotropy of the orbital moment—that is, of the expectation value of L_z [8,9]. The correct comparison to low temperature measurements ($T \rightarrow 0$ K) of the MAE according to Eq. (1) could not be performed.

In this work we will measure in a new way via only one experimental technique, that is, frequency- and angular-dependent ferromagnetic resonance (FMR),

independently both MAE at $T \approx 0$ K and the orbital moment anisotropy for Fe monolayers. We find an about 300% increase of the ratio of orbital to spin moment $\mu_L/\mu_S = 0.133$ in comparison to bulk Fe and a small anisotropy of the orbital momentum which is correlated with the experimental MAE at $T = 0$ K. Both sides of Eq. (1) are experimentally measured. It is pointed out that our FMR provides comparable information on the orbital magnetic moment as XMCD experiments, however, with the advantage that FMR can be measured in the laboratory. In addition, relativistic band structure calculations yield the layer-resolved magnetic moments of Fe and V of this structure.

The determination of μ_L of bulk materials or thick films from the spectroscopic splitting g tensor via FMR and electron spin resonance goes back half a century [10]. Because of the quenched orbital moment the g value is close to the one of the free electron $g \approx 2$. Higher order perturbation theory mixes excited states into the ground state, so that g is slightly smaller or larger than “2” depending on the sign of the spin-orbit coupling being positive or negative [6,11]. For Fe, Co, and Ni one finds $g > 2$. The same admixture of excited states leads also to some anisotropy of μ_L yielding a g tensor in solids [11]. The deviation of the g value from 2 is a measure of the orbital contribution according to [10],

$$\frac{\mu_L}{\mu_S} = \frac{g - 2}{2}. \quad (2)$$

If μ_S or the total moment μ is known from theory or experiment, μ_L can be determined absolutely. Moreover, by determining the elements of the g tensor in different crystallographic directions, Eq. (2) yields the anisotropy of μ_L . The MAE has the same origin, that is, orbital magnetism [2,6,8,11,12]. Precision magnetometry measurements [6,13] and theoretical results for bulk Fe, Co, and Ni samples [2–5] indicate that the easy axis of magnetization is parallel to the direction with the largest μ_L .

In ultrathin films the easy axis is not determined by Eq. (1) alone. The shape anisotropy which arises from the dipole-dipole interaction may be larger than the intrinsic MAE [6,14] and force the magnetization parallel to the film plane. Also in this case the largest orbital moment is expected along the easy axis given by the orbital magnetism. In our notation μ_L^{\parallel} is the moment perpendicular to the film plane. Note that μ_L^{\parallel} and μ_L^{\perp} *a priori* are NOT related to in- and out-of-plane orientations in thin films.

In experimental work the MAE of thin films with tetragonal symmetry is calculated from experimentally determined phenomenological anisotropy constants K_2 , $K_{4\parallel}$, and $K_{4\perp}$ which are temperature dependent [6]. The MAE entering Eq. (1) must be obtained from the difference in the total energies between two crystallographic directions [14] evaluated at $T = 0$ K,

$$\text{MAE} = E_{[001]} - E_{[110]} = -K_2 - \frac{1}{2}K_{4\perp} + \frac{1}{4}K_{4\parallel}. \quad (3)$$

A prototype 3d-metal-based multilayer consisting of 2 monolayer (ML) Fe and 5 ML V was chosen, for which enhanced orbital magnetism is expected: a bcc(001) (Fe_2/V_5)₆₀ [15] single crystalline superlattice on MgO(001). Details about the sample preparation, structural, and magnetic characterizations have been published elsewhere [16–18]. The Fe/V(001) superlattices present an exceptionally high structural coherence [16] and magnetic homogeneity [18].

FMR measurements at 1.12, 4.06, and 9.24 GHz (see Fig. 1) are performed with the magnetic field applied in the film plane along [110] and perpendicular along [001]. For the parallel configuration the resonance condition is [14]

$$\frac{\omega^2}{\gamma_{\parallel}^2} = H_{r\parallel}^2 + H_{r\parallel} \left(4\pi M - 2 \frac{K_2}{M} - \frac{K_{4\parallel}}{M} \right) - 2 \frac{K_{4\parallel}}{M} \left(4\pi M - 2 \frac{K_2}{M} + \frac{K_{4\parallel}}{M} \right), \quad (4)$$

and for the perpendicular configuration,

$$\frac{\omega}{\gamma_{\perp}} = H_{r\perp} - \left(4\pi M - 2 \frac{K_2}{M} - 2 \frac{K_{4\perp}}{M} \right), \quad (5)$$

where $f = \omega/2\pi$ is the resonance frequency, $\hbar\gamma_{\parallel,\perp} = g_{\parallel,\perp}\mu_B$ is the gyromagnetic ratio in plane and out of plane, and M is the magnetization. From Eq. (4) the g factor g_{\parallel} is obtained by plotting f^2 as a function of $H_{r\parallel}$ (Fig. 1). The fit (solid line) is *independent* of the values of the magnetization and MAE constants. g_{\perp} is obtained from Eq. (5), which is linear with respect to $H_{r\perp}$. Only frequency-dependent measurements [14,19,20] yield the necessary precision to extract anisotropic g values. In comparison to XMCD experiments FMR offers the unique advantage that it truly measures the magnetic ground state (excitations of spin waves with $k \approx 0$) and detects a signal also in the paramagnetic state above T_c where the XMCD signal vanishes.

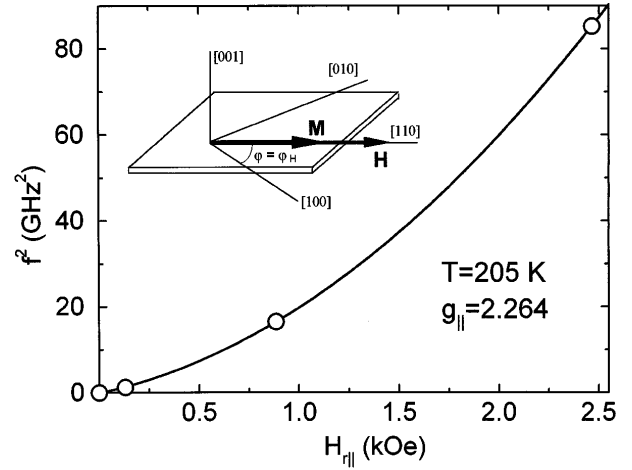


FIG. 1. Analysis of g_{\parallel} according to Eq. (4) at $T = 205$ K. The solid line is a fit to the experimental $H_{r\parallel}$ (circles).

The g -tensor elements g_{\parallel} and g_{\perp} were measured between 70–220 K ($T_c \approx 200$ K). The magnetic moment/atom—by definition—is temperature independent, that is, μ_L/μ_S and the g tensor are constant as confirmed by our measurement. As listed in Table I we find an average $g = 2.266$ which is significantly larger than $g = 2.09$ of bulk Fe [13] and other Fe films [14,19,20]. With Eq. (2) we find $\mu_L/\mu_S = 0.133$ for the Fe/V interface, which in the atomic model can be regarded as a Fe-V pair due to the strong coupling. There is also a small difference of the g values in- and out-of-the-film plane: $g_{\parallel} = 2.264$ and $g_{\perp} = 2.268$. That is to say, the orbital magnetism is nearly isotropic. This is unexpected for a 2 ML Fe(001) layer, but as shown below it is fully consistent with the measured small bulklike MAE (Table I). To determine μ_L absolutely we calculate the spin moment μ_S (Table I) self-consistently within the framework of density functional theory in its local density approximation. The computational technique is based on the linearized muffin-tin orbital method and the corresponding Green's function technique for surfaces and interfaces, as has been developed by Skriver and Rosengaard [21]. The calculated bcc(001) V/Fe₂/V₅/Fe₂/V(001) bcc system consists of two double layers of iron separated by five layers of vanadium embedded between two semi-infinite

TABLE I. Values of the g -tensor components in-plane (g_{\parallel}) and out-of-plane (g_{\perp}), average orbital and spin moments μ_L , μ_S , their ratio calculated from Eq. (2) and MAE for the Fe₂/V₅ superlattice and bulk Fe (from [13]).

bcc (001)Fe ₂ /V ₅ superlattice					
g_{\parallel}	g_{\perp}	μ_L/μ_S	μ_L (μ_B)	μ_S (μ_B)	MAE ($\mu\text{eV}/\text{atom}$)
2.264	2.268	0.133	0.126	1.62	-2.0
± 0.015	± 0.015				± 0.5
bcc Fe-bulk					
2.09	2.09	0.045	0.10(4)	2.13(5)	-1.4

vanadium bcc(001) crystals. The underlying lattice is that of bcc(001), where no local lattice relaxations are considered. The calculations are performed for two limiting cases: the lattice constant of the superlattice being equal to that of bulk Fe or of V. It is expected that volume conserving, tetragonal distortions usually have only a small influence on μ_S . The results for bcc(001) V/Fe₂/V₅/Fe₂/V bcc(001) are shown in Fig. 2. Note that V acquires a magnetic moment mostly located at the interface antiferromagnetically coupled to the Fe moment, in agreement with previous theoretical and experimental work [22]. In the following, all moments refer to the calculation performed with the Fe lattice constant. A spin moment of $1.62\mu_B$ for Fe and $-0.67\mu_B$ for V is found (Fig. 2). The reduced μ_S for Fe is attributed to hybridization effects at the Fermi edge of Fe in proximity to V [23]. This result is in reasonable agreement with previous SQUID measurements which yield a slightly smaller Fe moment, if one considers that the 2 ML layers are not perfect and 1 ML patches do carry only a negligible moment $\mu_S \approx 0.05\mu_B$ [17]. In the theoretical part only the spin moment was analyzed (Table I). For a proper analysis of the total moment one should not confuse total and spin moment [22], since the contribution of the orbital part can be enhanced significantly as shown here. We calculate $\mu_L = 0.126\mu_B$ for the Fe/V pair via Eq. (2). The separation of the Fe orbital moment alone is not possible. But it is reasonable to assume that it is enhanced in comparison to $\mu_L = 0.10\mu_B$ of bulk bcc Fe [12], since the moment of V at the interface has the opposite sign. For 3–4 ML of fct Fe on Cu(001) $\mu_L = (0.23-0.25)\mu_B$ have been determined via XMCD [24].

Let us now turn to the main point of this Letter: a critical experimental check of the relation between MAE and $\Delta\mu_L$. The anisotropy parameters K_i are determined with high precision by temperature- and angular- (azi-

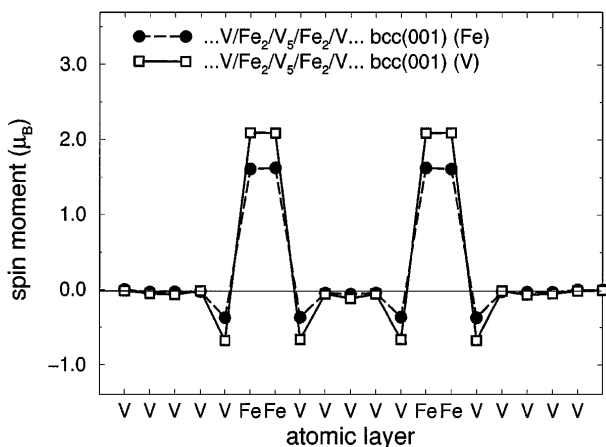


FIG. 2. Layer-resolved spin moments of Fe and V from first-principles calculation. Two results assuming the lattice constants of Fe (solid circles) or V (open squares) for the superlattice are shown.

muthal and polar) dependent FMR as discussed in detail elsewhere [14,18,25]. All K_i are temperature dependent [Fig. 3(a)]. At all temperatures we find that the magnetization lies in the film plane although the total MAE [Eq. (3)] is negative which favors the out-of-plane orientation [001]. This shows that the shape anisotropy dominates. $|K_{4\perp}|$ is comparable to the corresponding value of $1.4 \mu\text{eV}/\text{atom}$ for bulk Fe [13,14] and slightly smaller than K_2 . Both vanish close to $T_c \cong 200$ K. $K_{4\parallel}$ is about 1 order of magnitude smaller and vanishes at 100 K [18]. At first, the small values of K_2 are rather surprising for a sample with only two atomic layers of Fe in each superlattice period. If one attributes the K_2 mainly to the known Fe interface anisotropy, an orders-of-magnitude larger MAE would be expected [14]. Our finding shows that it makes no sense to discriminate between interface and volume anisotropy in a 2 ML thick ferromagnet. The magnetism of the Fe/V multilayer does not arise from the characteristics of the Fe atom alone, but the contribution from the V atoms at the interface is important. Note that the (Fe₂/V₅)₆₀ superlattice [15] contains only identical Fe/V interfaces. A detailed discussion of the origin of the temperature dependence of K_2 , $K_{4\parallel}$, and $K_{4\perp}$ is not the purpose of this Letter and has been published elsewhere [25]. Here we are interested in the total intrinsic MAE at $T = 0$ K which is the relevant quantity on the left-hand side of Eq. (1). This requires a determination

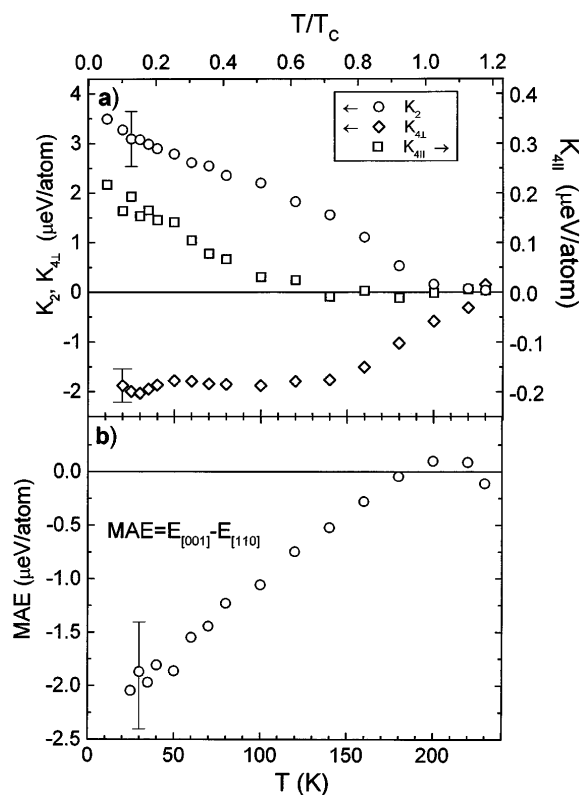


FIG. 3. (a) Temperature dependence of K_2 , $K_{4\parallel}$, and $K_{4\perp}$. Note the different scale for $K_{4\parallel}$. (b) Total magnetic anisotropy energy (MAE) for the Fe₂/V₅ superlattice according to Eq. (3).

of all K_i , that is, K_2 , $K_{4\perp}$, and $K_{4\parallel}$, at low temperatures (Fig. 3). With Eq. (3) and the data of Fig. 3(a) we calculate a surprisingly small MAE of $\approx -2 \mu\text{eV}/\text{atom}$ at $T = 0 \text{ K}$ as shown in Fig. 3(b). The total MAE changes as a function of T and vanishes near T_c . The orbital moment anisotropy, that is, g_{\parallel} and g_{\perp} , on the other hand, are temperature independent. This shows that FMR is capable of separating the effect of the microscopic orbital contribution from the macroscopic MAE of the whole sample which is tied to the magnetization. The comparison of MAE and $\Delta\mu_L$ is justified at $T = 0 \text{ K}$ only. Previous estimates [9] did not take the temperature dependence of MAE fully into account.

Now we are prepared to clarify the intimate relation between the intrinsic MAE and orbital magnetism in an itinerant ferromagnet. At first glance one might say that both have the same origin, namely, the second and third Hund's rule [6,11]. The first attempt to extend this local and intra-atomic picture to itinerant magnets [1] led to Eq. (1). Unfortunately this simple relation between MAE and $\Delta\mu_L$ was taken too seriously in that, e.g., $\Delta\mu_L$ was measured by means of XMCD and the MAE was "calculated" via Eq. (1). Bruno and coauthors stated already [3,4] that such a strict linearity does not exist. *Ab initio* calculations [2–4] have confirmed a more complicated nonlinear dependence. Here we present the first experimental independent determination of both sides of Eq. (1). In Table I the experimental values for the left-hand side of Eq. (1), i.e., the MAE $\cong -2 \mu\text{eV}/\text{atom}$ and for the right-hand side, i.e., $\Delta\mu_L = -3.2 \times 10^{-3} \mu_B$ are listed. The latter is calculated with Eq. (2) from g_{\parallel} and g_{\perp} . Substituting these values in Eq. (1) one obtains experimentally $\alpha \cong 0.05$. This compares well with the previous theoretical estimates for Co (0.2–0.25 [3]) and Ni (0.3–0.7 [2]). It is interesting to note that XMCD can determine only the right-hand side of Eq. (1) [9]. By FMR both sides may be measured in the laboratory, and orbital magnetism can be studied even above T_c in the same setup. These advantages together with its high sensitivity make FMR a powerful complementary technique to study orbital magnetism of ultrathin films and multilayers.

In conclusion, frequency-, angular-, and temperature-dependent FMR has been used to quantify the relation of anisotropic orbital moments and MAE for the first time. For a bcc(001) $(\text{Fe}_2/\text{V}_5)_{60}$ superlattice the spectroscopic splitting tensor (g tensor) is determined, and a 300% enhanced μ_L/μ_S compared to bulk Fe is found. In combination with *first-principles* calculations we show that this is mainly due to a reduced spin moment at the Fe/V interface. The orbital moment perpendicular to the film plane is slightly larger than the one in plane which is consistent with the sign and magnitude of the intrinsic MAE at $T = 0 \text{ K}$. The total magnetization, however, has its easy axis in plane due to the dominance of shape anisotropy caused by the magnetic dipole-dipole interaction.

This work was supported in part by the DFG, Sfb 290 and the Swedish Material Consortium No. 9 and NFR Grant No. 9871-321. The sample was prepared within the Thin Film Consortium. Financial support from NUTEK is also acknowledged.

*Corresponding author.

Electronic address: babgroup@physik.fu-berlin.de

†New address: Department of Materials and Chemical Engineering, ABB Corporate Research, S-72178 Västerås, Sweden.

- [1] P. Bruno, Phys. Rev. B **39**, 865 (1989); in *Ferienkurse des Forschungszentrum* (Jülich, Jülich, 1993), Vol. 24, p. 24.
- [2] O. Hjortstam *et al.*, Phys. Rev. B **55**, 15 026 (1997).
- [3] B. Újfalussy, L. Szunyogh, P. Bruno, and P. Weinberger, Phys. Rev. Lett. **77**, 1805 (1996).
- [4] L. Szunyogh, B. Újfalussy, and P. Weinberger, Phys. Rev. B **51**, 9552 (1995).
- [5] Ruqian Wu, Lujun Chen, and A.J. Freeman, J. Magn. Mater. **170**, 103 (1997).
- [6] K. Baberschke, Appl. Phys. A **62**, 417 (1996).
- [7] *Spin-Orbit-Influenced Spectroscopies of Magnetic Solids*, edited by H. Ebert and G. Schütz, Lecture Notes in Physics Vol. 466 (Springer-Verlag, Berlin, 1996).
- [8] M. Tischer *et al.*, Phys. Rev. Lett. **75**, 1602 (1995).
- [9] D. Weller *et al.*, Phys. Rev. Lett. **75**, 3752 (1995).
- [10] C. Kittel, Phys. Rev. **76**, 743 (1949); A.J.P. Meyer and G. Asch, J. Appl. Phys. **32**, 330S (1961), and references therein.
- [11] A. Abragam and B. Bleaney, in *Electron Paramagnetic Resonance of Transition Ions* (Clarendon Press, Oxford, 1970), and similar textbooks.
- [12] I. V. Solov'yev, A. I. Liechtenstein, and K. Terakura, Phys. Rev. Lett. **80**, 5758 (1998).
- [13] M.B. Stearns, in *Numerical Data and Functional Relationships in Science and Technology*, edited by H.P.J. Wijn, Landolt-Bornstein, New Series, Group 3, Vol. 19a (Springer-Verlag, Berlin, 1986).
- [14] M. Farle, Rep. Prog. Phys. **61**, 755 (1998), and references therein.
- [15] The notation $(\text{Fe}_2/\text{V}_5)_{60}$ commonly used in the literature means 2 ML Fe and 5 ML V layers with a repetition rate of 60.
- [16] P. Isberg *et al.*, Vacuum **48**, 483 (1997); P. Pouloupoulos *et al.*, J. Magn. Mater. **170**, 57 (1997).
- [17] L.-C. Duda *et al.*, Phys. Rev. B **54**, 10 393 (1996).
- [18] A. N. Anisimov *et al.*, J. Phys. Condens. Matter **9**, 10 581 (1997).
- [19] B. Heinrich *et al.*, Phys. Rev. B **38**, 12 879 (1988).
- [20] F. Schreiber *et al.*, Solid State Commun. **93**, 965 (1995).
- [21] H.L. Skriver and N.M. Rosengaard, Phys. Rev. B **43**, 9538 (1991).
- [22] M.M. Schwickert *et al.*, Phys. Rev. B **57**, 13 682 (1998).
- [23] S. Mirbt, I. A. Abrikosov, B. Johansson, and H.L. Skriver, Phys. Rev. B **55**, 67 (1997).
- [24] J. Hunter Dunn, D. Arvanitis, and N. Mårtensson, Phys. Rev. B **54**, R11 157 (1996).
- [25] A. N. Anisimov *et al.*, IEEE Trans. Magn. **34**, 873 (1998).